

4 Down, 50 to go – An Update on Harbor Surveys in the United States

Dr. Gregory W. Johnson, Ruslan Shalaev, Christian Oates; *Alion Science & Technology*
CAPT Richard Hartnett; *US Coast Guard Academy*
Prof. Peter F. Swaszek; *University of Rhode Island*

ABSTRACT

There has been interest in recent years in using Loran-C as a back-up system in case of the loss of GPS; especially in the Harbor Entrance and Approach (HEA) arena. The U.S. Coast Guard Academy, in conjunction with the U.S. Coast Guard Loran Support Unit, is conducting research and proof-of-concept demonstrations of the ability of enhanced Loran to support the HEA navigational requirements; specifically, the accuracy requirement. In order to meet this accuracy requirement, user receivers must employ Additional Secondary Factors (ASFs) in calculating the user's position. ASFs are time adjustments that modify the receiver's times of arrival to account for propagation over non-seawater paths. As these ASFs vary both spatially and temporally, both variations need to be accounted for to meet the accuracy targets.

In the proposed *e*Loran system, the spatial variations are accounted for through the use of grids of ASF values that are known by the receiver a priori. The temporal variations are accounted for by operating in differential mode; specifically, a nearby reference station estimates and broadcasts the temporal changes in the ASFs relative to the published spatial grids. In this paper, we outline the methodology that has been developed, review the data collection in the four harbors completed to date, describe our spatial ASF grid development techniques, and provide grid and performance examples from New York, New London (CT), Norfolk (VA), and Boston (MA) harbors.

INTRODUCTION

As defined in [1] “*enhanced Loran is an internationally standardized positioning, navigation, and timing (PNT) service*” for use by many modes of transport and in other applications. Due to its very different operation and failure modes, *e*Loran provides an ideal complement to Global Navigation Satellite Systems (GNSS) that allows users to retain the safety, security, and economic benefits of GNSS, even when their satellite services are disrupted. As a modernized Loran system, *e*Loran continues to be a low-frequency, terrestrial navigation system operating in the 90-kHz to 110-kHz frequency band synchronized to coordinated universal time. The primary difference between *e*Loran and Loran-C is the addition of a data channel. This data channel is used to transmit, among other things, station identification, absolute time, warnings of anomalous conditions, and differential corrections. This enables operations that satisfy the accuracy, availability, integrity, and continuity performance requirements for non-precision approach and harbor entrance and approach. It also meets the requirements of non-navigation time and frequency applications.

A great deal of effort has gone into analyzing and validating the suitability of Loran as a backup to GNSS/GPS. The culmination of several years worth of work by a team of experts from industry, academia, and government was the Loran Evaluation Team report [2]. This report “*shows that the modernized Loran system could satisfy the current Non-Precision Approach (NPA), Harbor Entrance and Approach (HEA), and timing/frequency requirements in the United States and could be used to mitigate the operational effects of a disruption in GPS services, thereby allowing the users to retain the benefits they derive from their use of GPS.*” Since the report was completed in 2004, the Loran Working Groups have focused on developing methodologies so that the *e*Loran system does indeed meet the requirements.

A significant factor limiting the position accuracy of Loran is the spatial and temporal variation in the times of arrival (TOAs) observed by the receiver. These variations are mostly due to the signals

propagating over paths of varying conductivity and topography (different from seawater). The TOA corrections which compensate for non-seawater paths are called additional secondary factors (ASFs). The Harbor Entrance and Approach (HEA) navigation strategy proposed by the Loran ASF Working Group achieves the required accuracy (8-20m) by removing the ASFs from the Loran signal time-of-arrival data before the position solution. Typically, we think of the ASF as consisting of two components which will be dealt with separately:

- the spatial term – it is envisioned that this component is tabulated as an ASF “grid” that is interpolated (possibly in a bootstrapping, iterative way as discussed in [3]) to identify the value for removal. Research issues include determining the required grid density, defining the regions of interest, and developing the best methods of grid creation and description.
- the temporal term (possibly with strong diurnal and seasonal characteristics) – it is envisioned that this component (or at least a large part of it) is removed by subtracting out the equivalent temporal term measured at a nearby Loran monitor site and broadcast over the Loran Data Channel (LDC). Current research issues on this approach include determining the correlation distance of the monitor site, methods for “smoothing” the ASF measurements at the monitors, and developing techniques to combine temporal terms from multiple monitor sites (see [4]).

The authors have been investigating these issues and working to develop a methodology for harbor ASF grid survey procedures and implementing *e*Loran for HEA. We have reported on these developments previously in [5-8]. In this paper we will first outline the methodology that has been developed and review the data collection in the four harbors completed to date. Then we will discuss our technique for converting measurements into a spatial grid and provide performance examples from the four harbors. We also discuss the LDC architecture for live broadcast of differential corrections to handle the temporal ASF corrections.

HARBOR SURVEY METHODOLOGY

The harbor survey methodology has been developed, tested, and refined over the course of the past year while completing four harbor surveys. There are four components of the methodology: the pre-survey planning, the field test, the data reduction, and the grid generation.

The pre-survey planning is to identify the HEA area and generate sail plans that will cover all of the areas of interest. Defining the HEA area is more a policy or operational decision than a technical one; however, we have not been able to find a definitive statement as to what constitutes the HEA area. In the absence of guidance we have made the assumption that the harbor area constitutes the white areas on the nautical chart (the main shipping channels and deep water) and that the approach area is within 6-8 NM of the approach buoy. In general, the area to be surveyed needs to over-bound the HEA area; survey tracks must be planned on both the inside and outside edges of all channels. In all areas of interest multiple tracks are needed, with typically 200m spacing to enable grids to be created at a 500m spacing.

The second step is to conduct the field test itself. During the course of the test, a static monitor must be installed somewhere in the harbor area. This is used to remove the temporal variation from the ASF measurements during the course of the survey. Since the spatial grid is relative to the location of the monitor site, this should be in the location where the final harbor monitor will be placed. Data collection is then performed throughout the harbor following the pre-planned routes measuring TOAs, ASFs, and GPS position.

The third step is the data reduction. During the data collection raw GPS pseudoranges are recorded. These are post-processed using data from local CORS sites to generate a precise GPS track with decimeter accuracy. The measured TOAs are corrected in post-processing for the velocity vectors of the vessel in the direction of each Loran tower and for the slight rotational effect of the H-field antenna using an algorithm that we developed and tested. New, more precise ASFs are then calculated using the corrected TOAs and the precise GPS track. The precise ASFs are converted to relative ASFs (relative to the monitor location) by subtracting the monitor site ASFs at the corresponding times.

This eliminates any temporal variations (due to daily, seasonal, weather, or system timing effects) from the measurements. The final step in the processing is to use the calibration tracks to remove any bias and align the data sets from day to day.

The fourth and final step is the creation of the ASF grid from the tracks of relative ASFs. This will be discussed in the section below. This procedure has been tested and refined in four harbors: New London, New York, Norfolk, and Boston.

NEW YORK PHASE I

New York harbor was split into several phases. Phase I focused on the upper harbor area (north of the Verrazano Bridge). At this stage of methodology development we were testing whether continuous vessel tracks were acceptable or whether we needed to do static measurements, so both were done. The CG Auxiliary vessel *Launch #5* (Figure 1) was used for the on-water measurements. The vessel tracks for the three days for measurements are shown in Figure 2. The bearings to the four strongest Loran stations are indicated by the red arrows. The harbor monitor site was installed at the Coast Guard ESD building on Staten Island (indicated by a black cross). The relative ASFs for Nantucket are shown in Figure 3. In this figure you can see that the Nantucket ASF increases north of Staten Island.



Figure 1: Survey vessel for NY Phase I: CG Auxiliary vessel *Launch #5*.

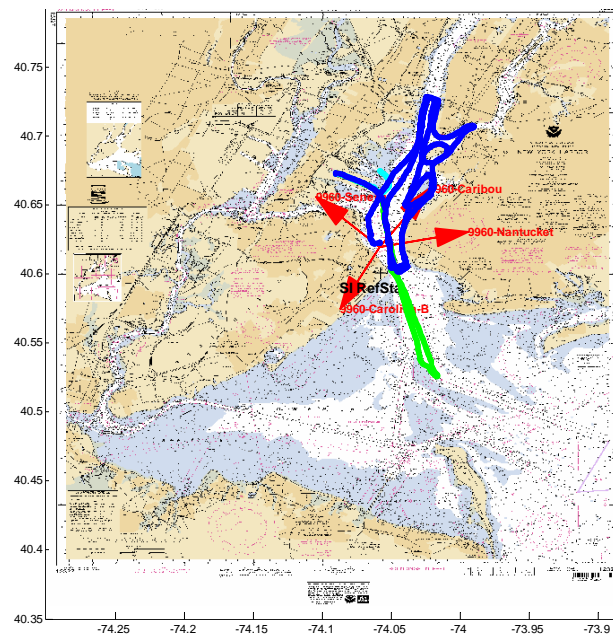


Figure 2: NY Phase I vessel tracks.

The survey vessel was also used to collect data at 25 static locations in the harbor; these 44 points are shown in Figure 4. For these points the vessel held station next to a buoy or pier for 10-15 minutes. The Loran van (Figure 5) was used to collect data at 19 static locations around the harbor on piers and other points near the water. For these points data was collected for about 30 minutes.

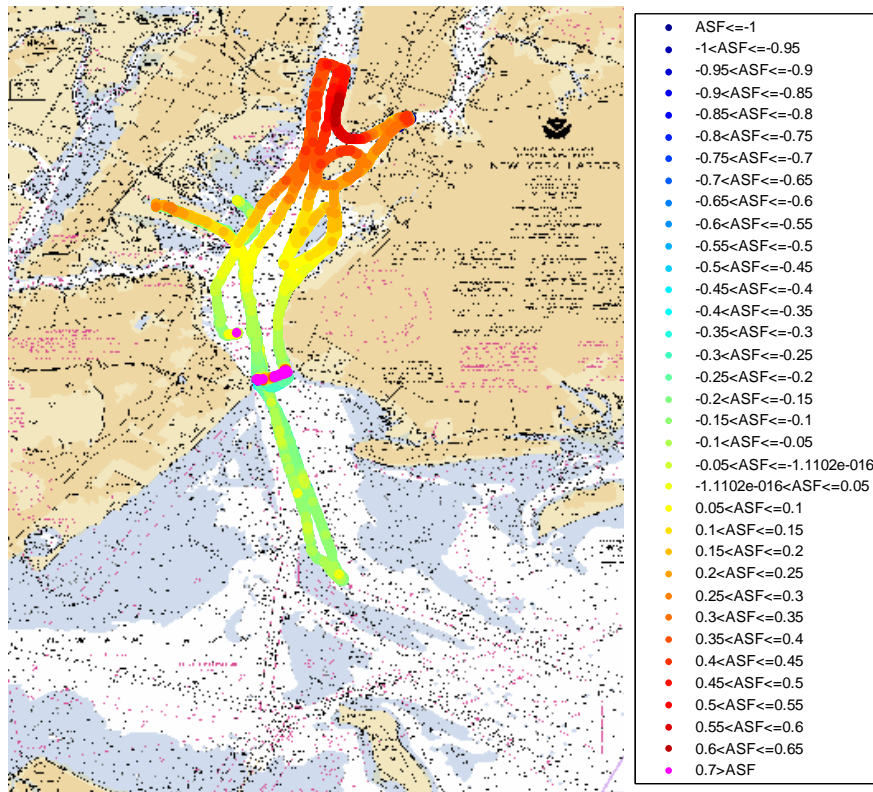


Figure 3: NY Phase I - Nantucket relative ASFs.

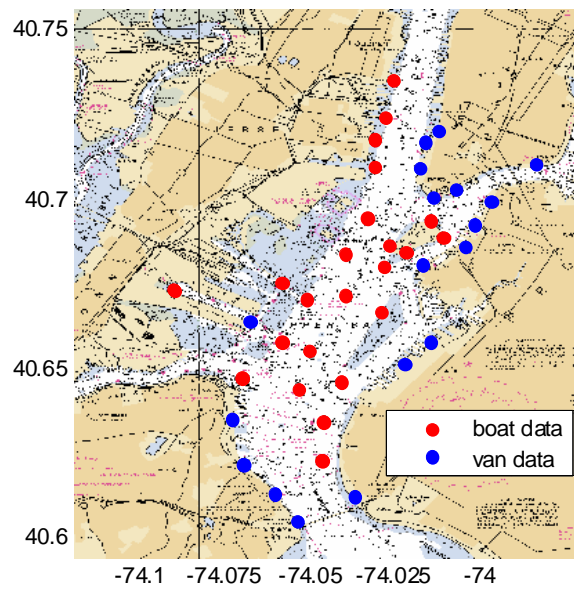


Figure 4: Vessel and van static points around NY Harbor.



Figure 5: Loran van in action in New York.

NEW YORK PHASE II

New York Phase II extended the survey area into the lower harbor as well as repeating the upper harbor for verification. The previous vessel was not available, so a commercial vessel, the *Jeanne II* (Figure 6), was hired. The vessel tracks for the three days of measurements are shown in Figure 7. The bearings to the four strongest Loran stations are indicated by the red arrows. The Harbor monitor site was installed and left at Staten Island (indicated by a black cross). The relative ASFs for Nantucket are shown in Figure 8. Once again, in this figure you can see that the Nantucket ASF increases north of Staten Island and decreases the farther south the vessel went.



Figure 6: NY Phase II vessel *Jeanne II*.

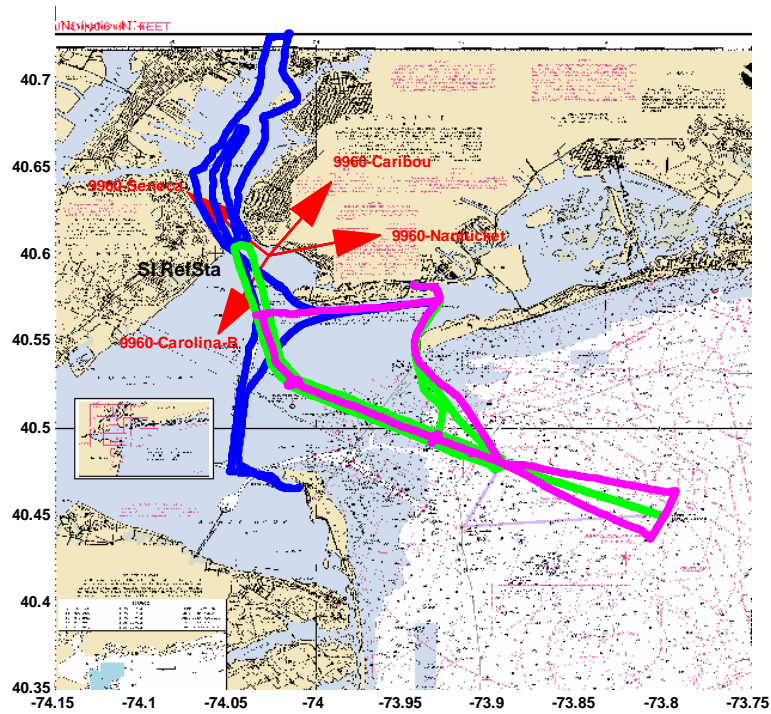


Figure 7: NY Phase 2 vessel tracks over 3 days (8/22 – magenta, 8/23 – green, 8/24 – blue).

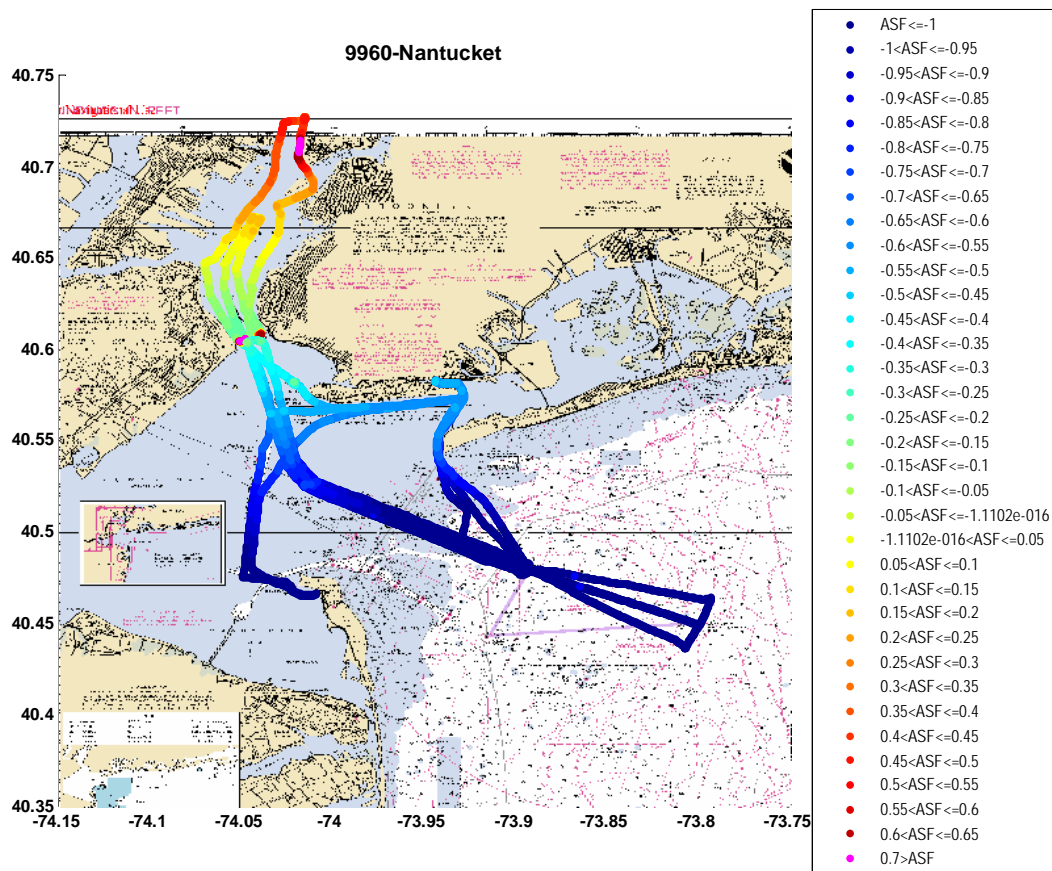


Figure 8: NY Phase 2 relative ASFs for Nantucket.

THAMES RIVER

We have done extensive work in New London harbor, which is basically the lower end of the Thames River in CT, as it is adjacent to our home base at the Coast Guard Academy. We have used several vessels for on-water measurement as well as the Loran van for shore-side measurements, but all of the more recent work has been done with the CG AUX vessel *Myst* (Figure 9). The entire river south of the Academy has been surveyed (see Figure 10). Again, the bearings to the four strongest Loran stations are indicated by the red arrows. The Harbor monitor site was installed at the Coast Guard Academy in New London (indicated by a black triangle). The relative ASFs for Nantucket and Seneca are shown in Figure 11. In this figure you can see that the Nantucket ASFs vary much more than those from Seneca.



Figure 9: CG Auxiliary vessel *Myst*.

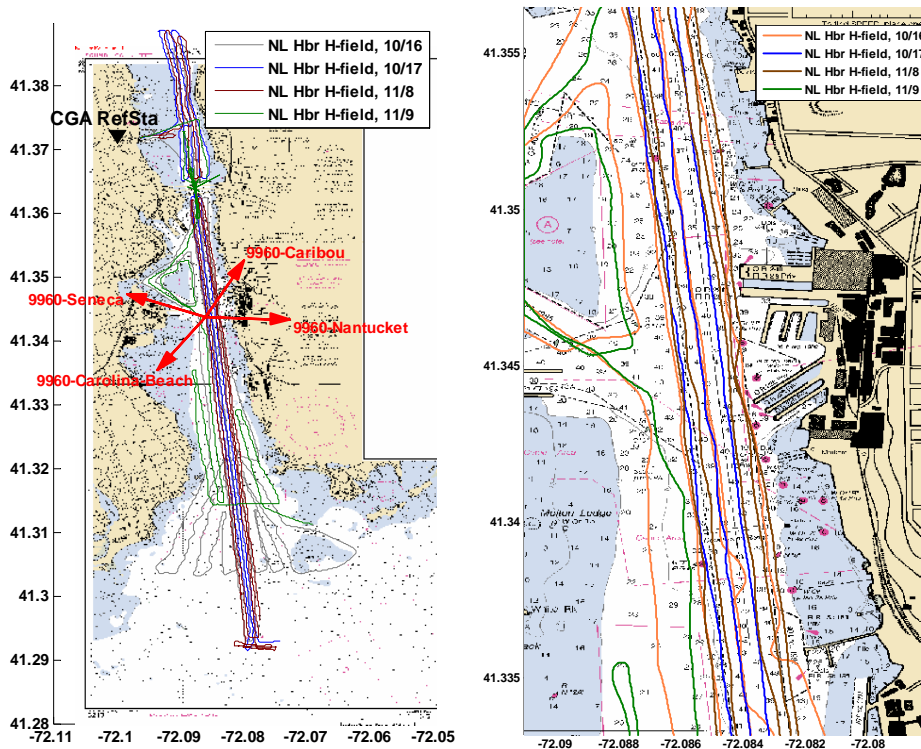


Figure 10: Thames River vessel tracks.

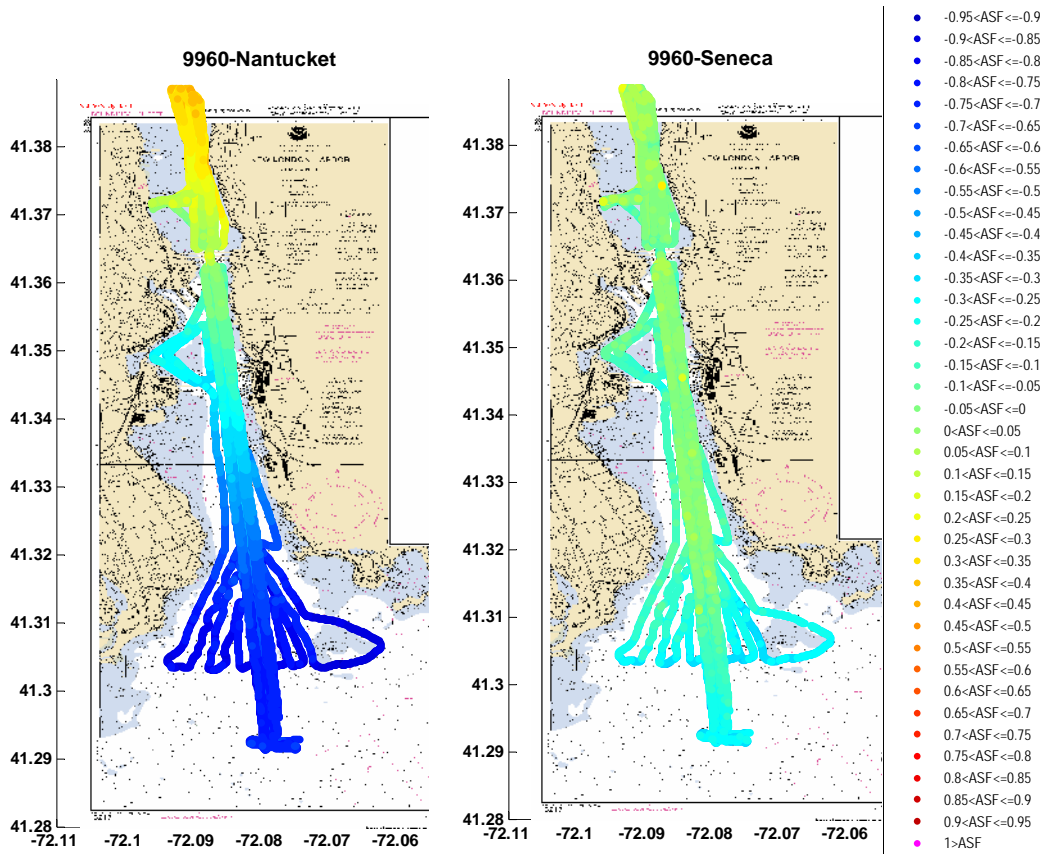


Figure 11: Thames River relative ASFs for Nantucket (left) and Seneca (right).

NORFOLK HARBOR

The third harbor surveyed was Norfolk Harbor. For this work we used the CG AUX vessel *Halcyon Lace* (Figure 12). Norfolk Harbor and the Chesapeake Bay are a huge area, so a subset was outlined for this survey; basically the main channel (Thimble Shoals Channel) from the entrance buoy all the way to the Hampton Bridge-Tunnel and then into the Norfolk Harbor area. This area was surveyed over 4 days (see Figure 13). Again, the bearings to the four strongest Loran stations are indicated by the red arrows. The Harbor monitor site was installed for the survey at the Coast Guard Station in Little Creek (indicated by a red triangle). The relative ASFs for Seneca are shown in Figure 14.



Figure 12: Norfolk Harbor survey vessel *Halcyon Lace*.

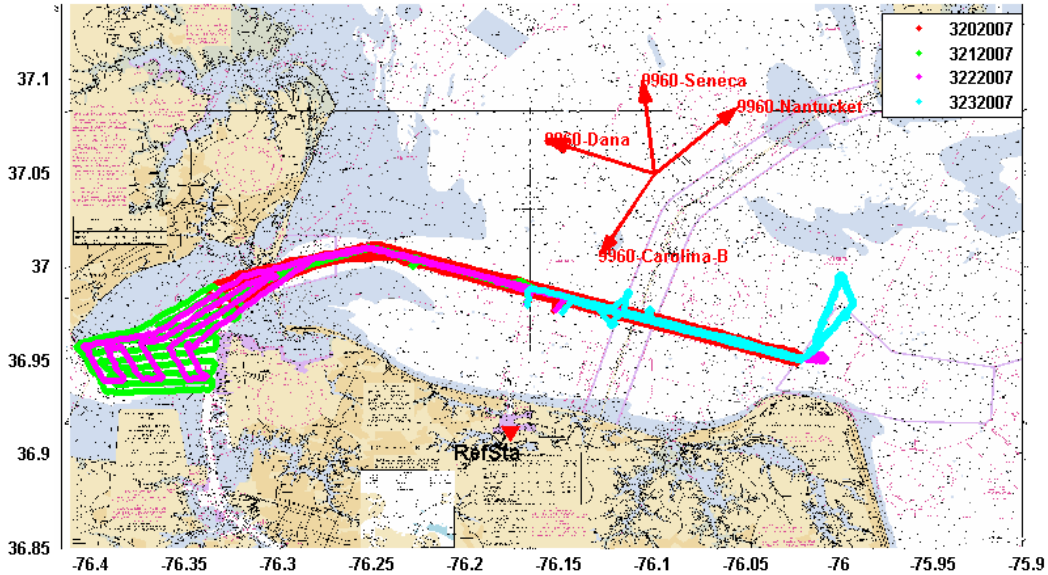


Figure 13: Norfolk Harbor vessel tracks over 4 days.

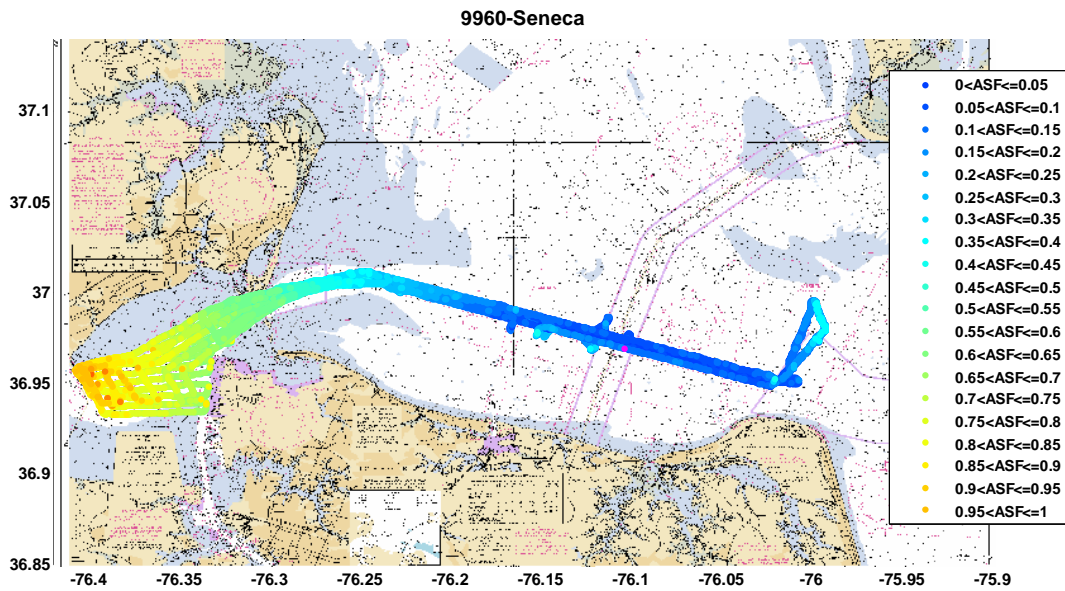


Figure 14: Norfolk Harbor relative ASFs for Seneca.

BOSTON HARBOR

The final harbor surveyed was Boston Harbor. For this work we used the CG AUX vessel *Three J's* (Figure 15). Sail plans were developed to cover a large area around the approach buoy, both channels (North and South) and the harbor area as far in as the CG Base. This area was covered over 3 days (see Figure 16). Here, the bearings to the seven strongest Loran stations are indicated by the red arrows. The harbor monitor site for the survey is the Seasonal Monitor site installed at the Volpe Transportation Systems Center in Cambridge, MA (indicated by a red triangle). The relative ASFs for Nantucket are shown in Figure 17.



Figure 15: Boston Harbor survey vessel *Three J's*.

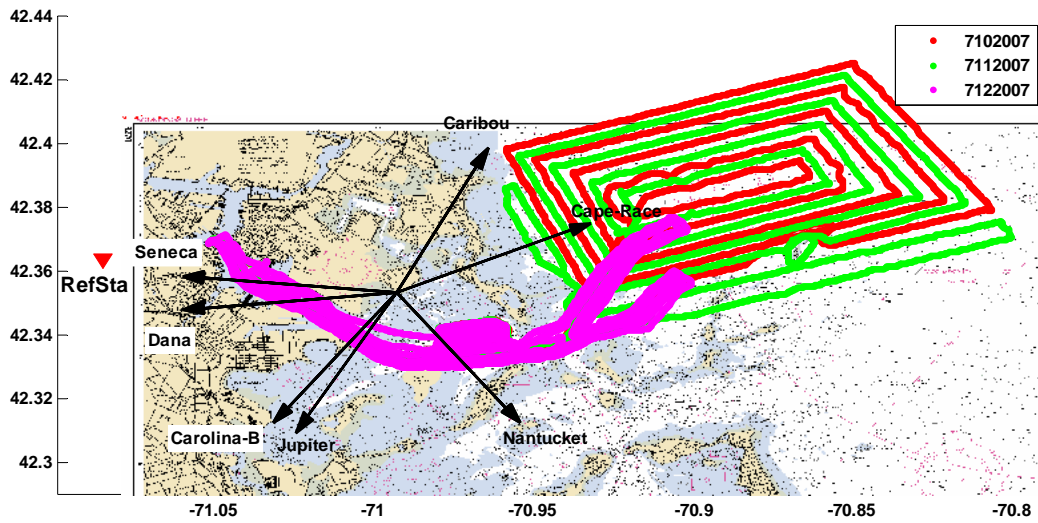


Figure 16: Boston Harbor survey tracks over 3 days.

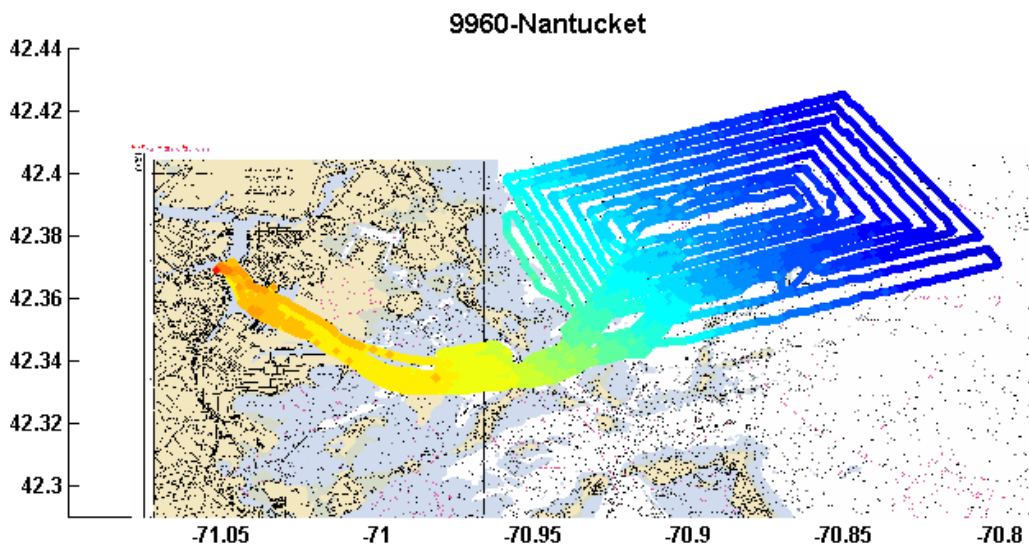


Figure 17: Boston Harbor relative ASFs for Nantucket.

SPATIAL ASF GRIDS

To remove the spatial component, our methodology assumes that a set of ASF grids is published for the HEA area (one grid for each Loran station). The user receiver then interpolates, based upon the user's estimated location, this grid to arrive at the ASF values to be used in the position solution. We briefly describe below our "inverse interpolation" technique (described in greater detail in [5, 6]) for creating spatial ASF grids from measured ASF data collected while cruising the harbor. The advantages of this technique are that the geometry of the data (location within the harbor) is explicitly used, there is an implicit correlation between adjacent grid points, and fewer grid points are missing in the result.

GRID DEVELOPMENT

Currently we employ an "inverse interpolation" method to generate a rectangular spatial grid of ASF values ASF from the relative ASF values.

- For a given latitude/longitude grid (for example, points on multiples of 0.0025 degrees) we compute the relative location of each data point within the grid. Specifically, we compute the proportional distances into the relevant grid cell (cell j,k , the one containing the desired location – see Figure 18) as

$$a = \frac{x - x_j}{x_{j+1} - x_j} \quad \text{and} \quad b = \frac{y - y_k}{y_{k+1} - y_k}$$

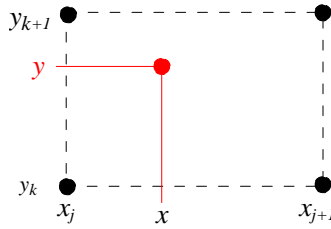


Figure 18: Standard interpolation – the a and b values are the fractional distances into the cell from the lower left corner.

- Next, we write the bilinear interpolation equation for each location

$$F(x, y) = (1-a)(1-b)F(x_j, y_k) + a(1-b)F(x_{j+1}, y_k) + b(1-a)F(x_j, y_{k+1}) + abF(x_{j+1}, y_{k+1})$$

in which the left hand side (the relative ASF) and the four coefficients on the right hand side are known; the result is a linear equation in the four ASF grid values (the unknowns) at the corners of the cell. For N locations, we end up with N simultaneous linear equations in the grid values. In matrix form, this is

$$A\mathbf{x} = \mathbf{b}$$

in which A is a matrix of the coefficients on the right hand sides of the equations above (and depends solely on the true position of the data measurements), \mathbf{b} is the vector of relative ASFs, and \mathbf{x} is a vector of the (unknown) grid values of interest.

- Solve the simultaneous linear equations for the ASF grid values using standard least squares techniques

$$\mathbf{x} = (A^T A)^{-1} A^T \mathbf{b}$$

The advantages of this method are (1) the explicit use of the location of each measurement in the grid value calculation and (2) the implicit coupling or correlation in the resulting ASF grid values since each relative ASF measurement contributes to the solution of all of the grid values.

The right hand portion of Figure 19 shows the 0.0025 degree ASF grid resulting from processing of the data in the left hand portion of Figure 19. We note that while we actually started computation with a rectangular grid, parts of the river (and adjacent land) have no grid values shown since the survey data did not cover that area; hence, no ASF estimates were generated. (If there is no survey data in the cells directly adjacent to a grid value, the least squares method interprets the problem as rank deficient and ignores that grid value variable in its solution.)

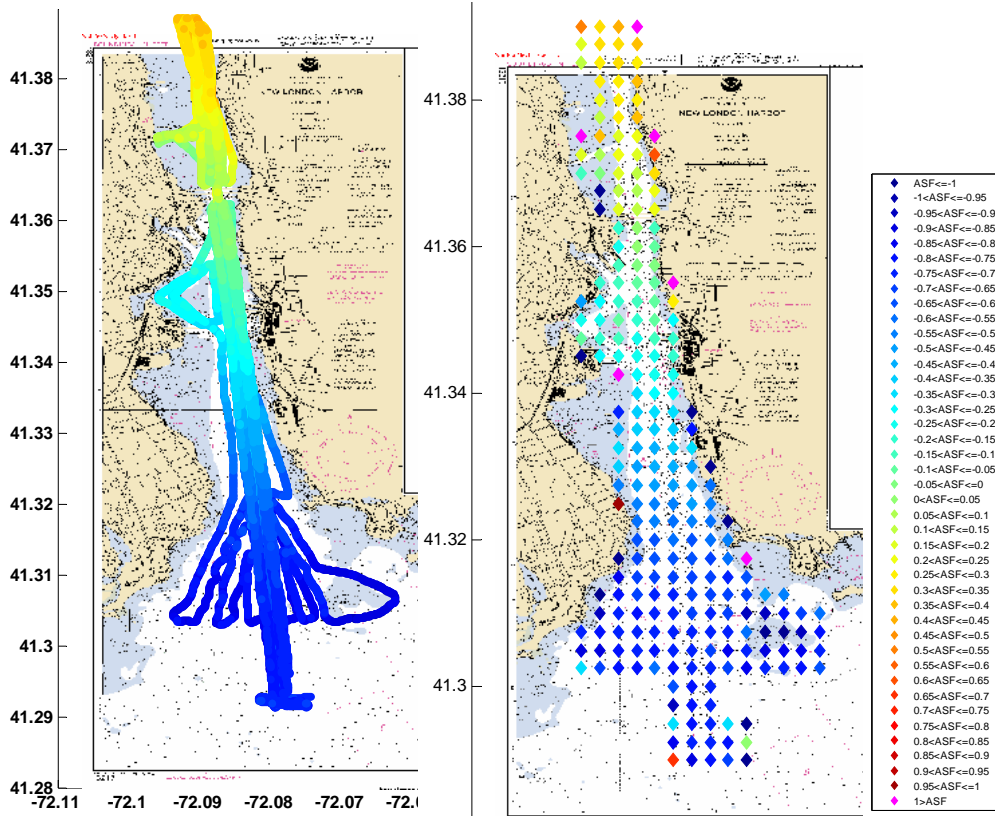


Figure 19: Relative ASFs (left) and the 0.0025 degree relative spatial ASF grid (right) for Loran station Nantucket on the Thames River.

GRID DENSITY

A natural question to ask when generating these grids is “*How well does the grid model the original data?*” To assess this, Figure 20 and Figure 21 show the relative ASF versus time of several north/south tracks on the lower portion of the Thames River for each of the three primary Loran stations observable: Seneca, Nantucket, and Carolina Beach, respectively. (As might be deduced from the figures, it was the sequence up, down, up, down, and up the river; each segment generating 2000+ samples.) In each figure the blue line is the relative measured ASF and the red line is the value interpolated from that station’s 0.0025 degree grid; also provided on each graph is the standard deviation of the difference between these two to measure the “fit”. When comparing these three figures, we note that the fit is better (i.e. the standard deviation is smaller) for stronger Loran signals (due to their relative distances, Nantucket if quite strong on the Thames, Seneca is next in received signal strength, and Carolina Beach is quite weak). Of significance is that the interpolated value (red) appears to closely track the center of the spread of each of these measurements.

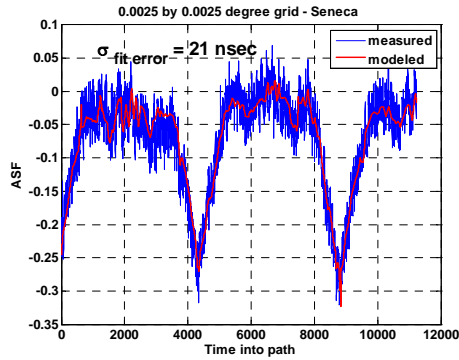


Figure 20: The “fit” of the 0.0025 degree relative spatial ASF grid for Loran station Seneca.

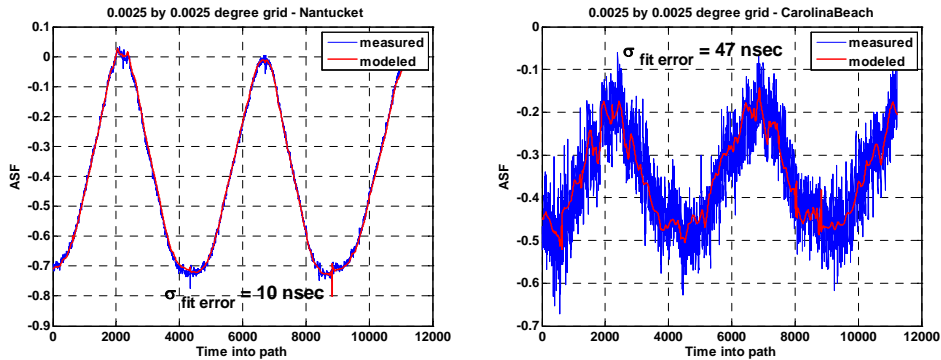


Figure 21: The “fit” of the 0.0025 degree relative spatial ASF grid for Loran stations Nantucket (left) and Carolina Beach (right).

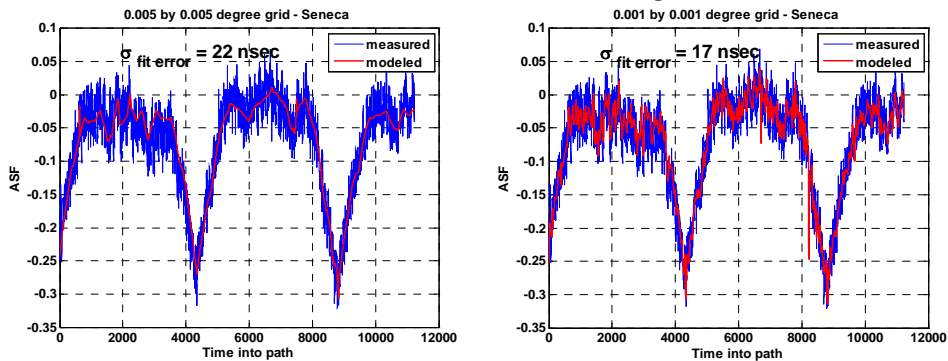


Figure 22: The “fit” of relative spatial ASF grids for Loran station Seneca: left, 0.005 degree; right, 0.001 degree.

A second question relating to ASF spatial grid development is “*How fine does the grid need to be*” or “*How do these fits vary with grid size?*” As a first assessment, Figure 22 shows the fits for the Seneca tracks on the Thames (compare to Figure 20) for two other grid sizes; a coarser resolution grid (0.005 degree spacing) and a finer resolution (0.001 degree), respectively. We note from the first subfigure that a coarser grid visually seems to yield a slightly poorer result; while the red line follows the blue data, it appears somewhat *rough* in responding to the ASF variation. Of course, much of the variation in the data itself is due to noise and we don’t want our grids to follow the noise. The second subfigure shows the other extreme; a grid that is *too* closely tracking the noise in the original survey data. By making the grid finer and finer, we can over-parameterize the problem and converge toward a “perfect” fit.

Table 1 shows the standard deviation metric of the differences for all three of these stations for a variety of grid resolutions. Based upon our experience to date, a 0.0025 to 0.005 degree grid (grid point spacing on the order of 300-500 meters) appears to be sufficient for HEA-capable ASF spatial

grids. (The table’s data suggests that the 0.0025 and 0.005 degree grids are nearly equivalent in quality.) The only time that a finer resolution might be appropriate is when the area of interest (and hence, the survey area) is small as may occur in a narrow channel. Specifically, for robustness of the inverse interpolation solution, we postulate that the grid resolution should be selected so that the area of interest is always several grid cells both in latitude and longitude.

Table 1: Comparison of the “fit” of various grid resolutions (resolution in degrees).

Resolution	~meters	Fit error in nsec		
		Seneca	Nantucket	Carolina Beach
0.0005	55	13	3	30
0.0010	110	17	7	40
0.0015	165	20	9	44
0.0020	225	21	10	47
0.0025	280	21	10	47
0.0050	560	22	10	48

GRID PERFORMANCE EXAMPLES

When assessing spatial grids, the best test of grid quality is to examine the resulting accuracy performance of the computed position of a receiver using these grids. For the results described here, this was done in a post-processing mode. This has been done for each of the four harbor areas. In each case, we have selected a single track portion in the grid area, shown in red in each figure (Thames River – Figure 23, New York – Figure 26, Norfolk – Figure 29, and Boston – Figure 32). When computing the e Loran positions, we included precise knowledge of the temporal correction at the monitor site so that this would not influence the examination of grid performance. For each case the first figure shows the error versus time and a histogram of the e Loran error for the segment and the next shows the scatter plot of the error to show its directional components.

For the Thames River, we note that the errors are always below the 20m target and, in fact, 95% of the time, the error is less than 10 meters. Figure 25 shows the scatter plot of the error to show its directional components. The arrows in Figure 23 show the crossing angles of the 3 signals used. The difficulty in the New London area is that the two strongest stations (Nantucket and Seneca) are almost opposite each other. The third station (Carolina Beach) is much weaker. As expected, this low received signal strength of the Carolina Beach signal causes the error scatter to have a strong north/south component. The size of the 95% error circle is thus very sensitive to the receiver tracking performance of Carolina Beach.

The second performance example is from New York. We note that once again the errors are always below the 20m target and, in fact, 95% of the time, the error is less than 8 meters. Figure 28 shows the scatter plot of the error to show its directional components. The arrows in Figure 26 show the crossing angles of the 3 signals used; here the good geometry of Loran towers in this vicinity and their near equal signal strengths yielded a satisfying “circular” error scatter.

The third performance example is from Norfolk, VA. We note now that the errors are *mostly* below the 20m target, although in this harbor performance is worse than the two examples above. Figure 31 shows the scatter plot of the error to show its directional components. The arrows in Figure 29 show the crossing angles of the signals used. In this harbor, the SNR from the stations is below that of the previous two examples (Carolina Beach is the only strong signal) which leads to more noise in the position solution as can be seen in the scatter plot.

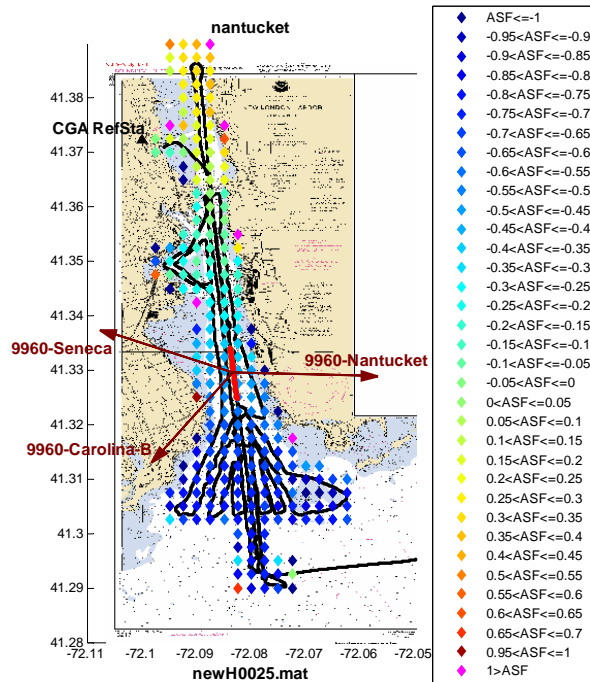


Figure 23: The Thames River grid for Nantucket with track segment used for analysis shown in red.

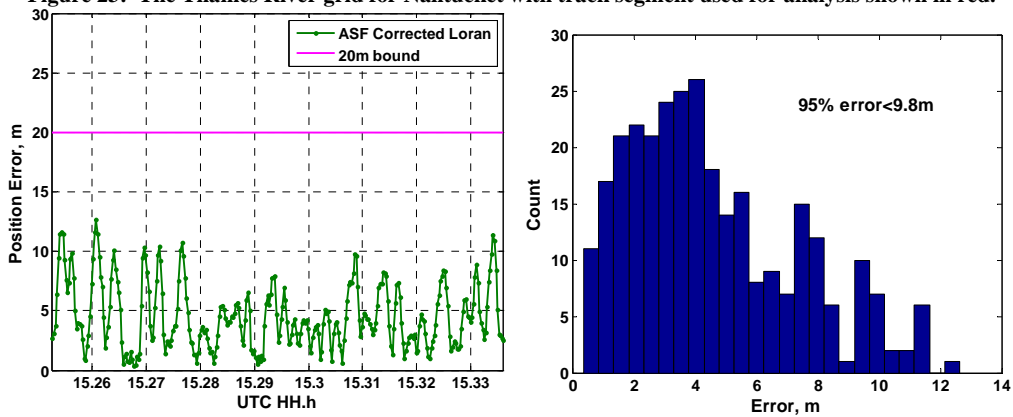


Figure 24: Accuracy results for the Thames River segment: left, error versus time; right, histogram of errors.

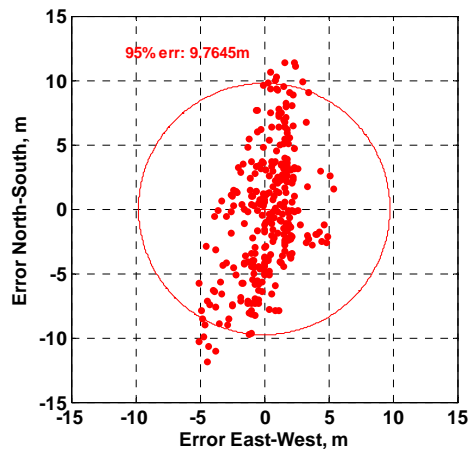


Figure 25: Error scatter plot for the Thames River segment showing sub 10m error 95% of the time.

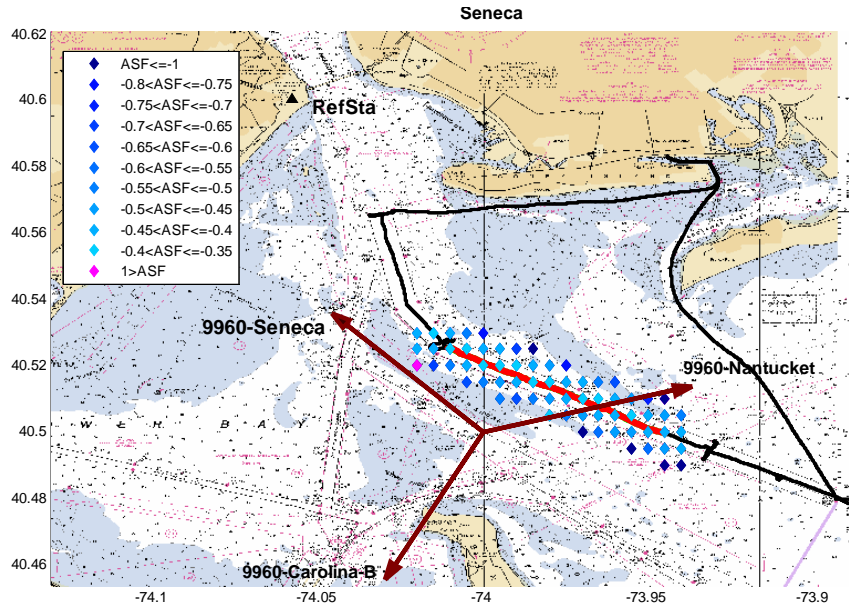


Figure 26: The New York harbor grid for Seneca with track segment used for analysis shown in red.

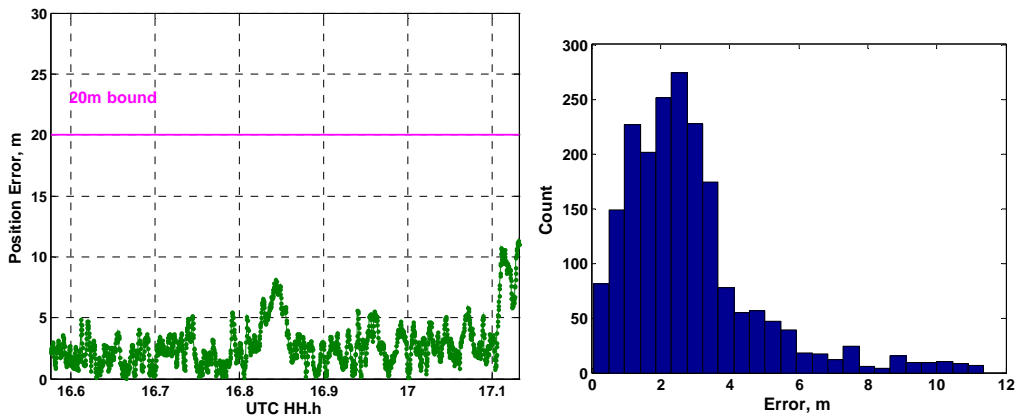


Figure 27: Accuracy results for the New York harbor segment: left, error versus time; right, histogram of errors.

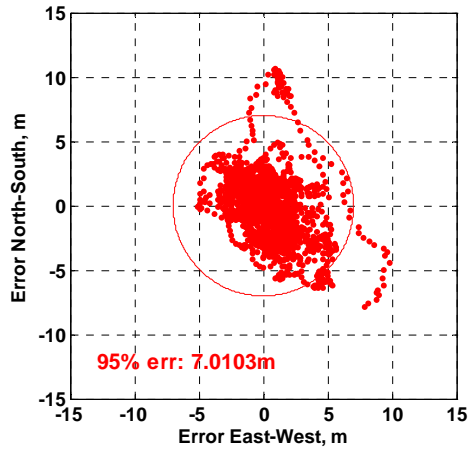


Figure 28: Error scatter for New York harbor test showing sub 7m error 95% of the time.

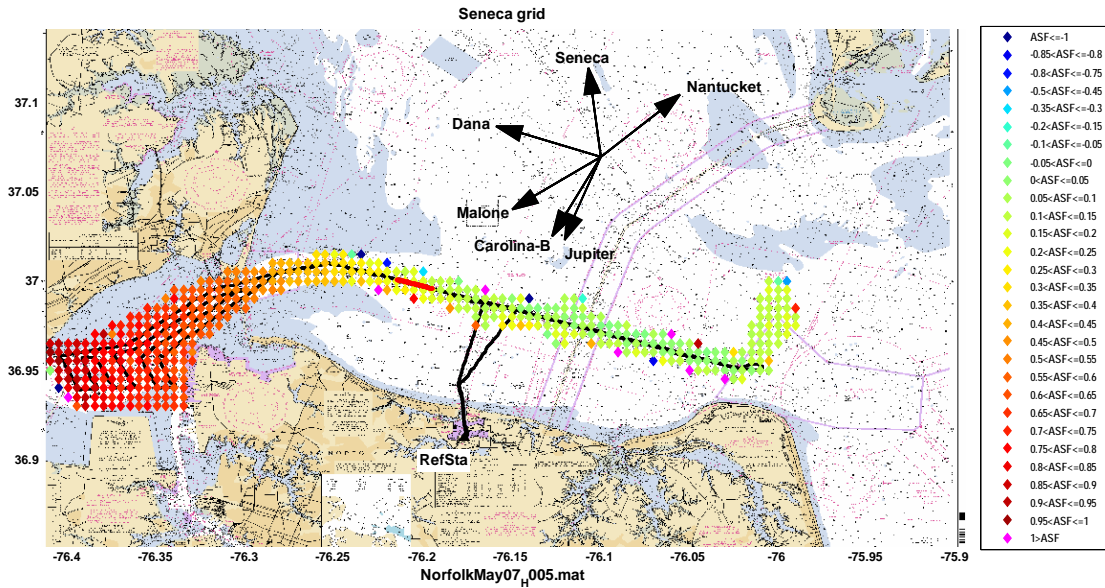


Figure 29: The Norfolk harbor grid for Seneca with track segment used for analysis shown in red.

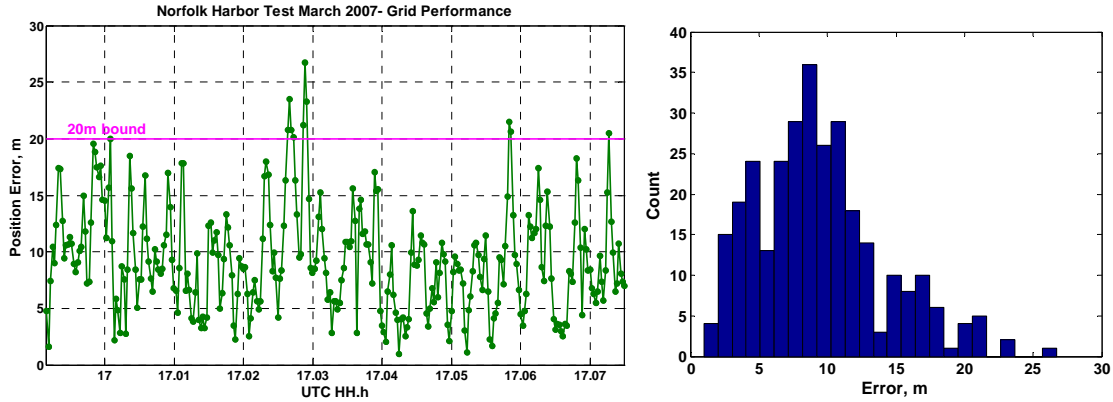


Figure 30: Accuracy results for the Norfolk harbor segment: left, error versus time; right, histogram of errors.

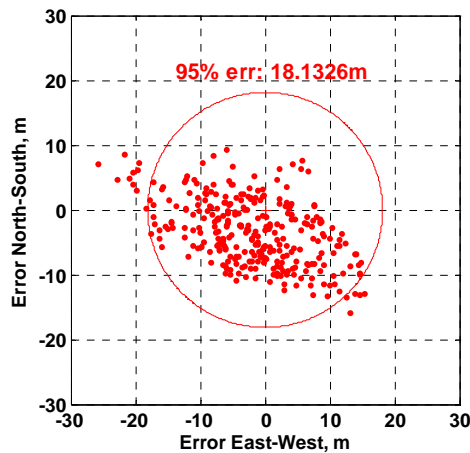


Figure 31: Error scatter for Norfolk harbor test showing sub 18m error 95% of the time.

The final performance example is from Boston. We note that once again the errors are always below the 20m target and, in fact, 95% of the time, the error is less than 8 meters. Figure 34 shows the scatter plot of the error to show its directional components. The arrows in Figure 32 show the crossing

angles of the 4 signals used; here the good geometry of Loran towers in this vicinity and good signal strength (near equal for 3 of the stations, with Nantucket being 10dB stronger than the other 3) yielded a mostly “circular” error scatter with a slight flattening in the direction of Nantucket.

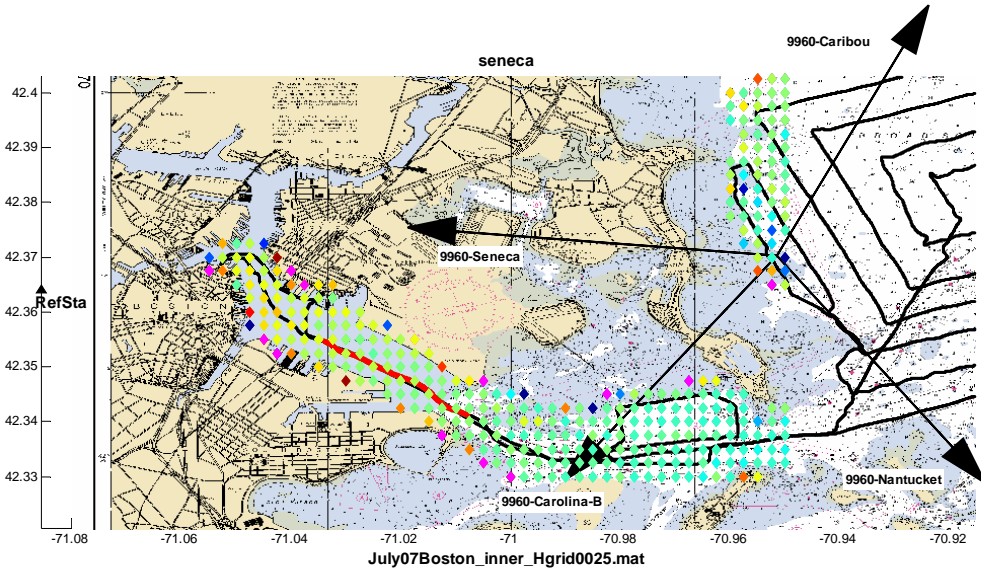


Figure 32: The Boston Harbor grid for Seneca with track segment used for analysis shown in red.

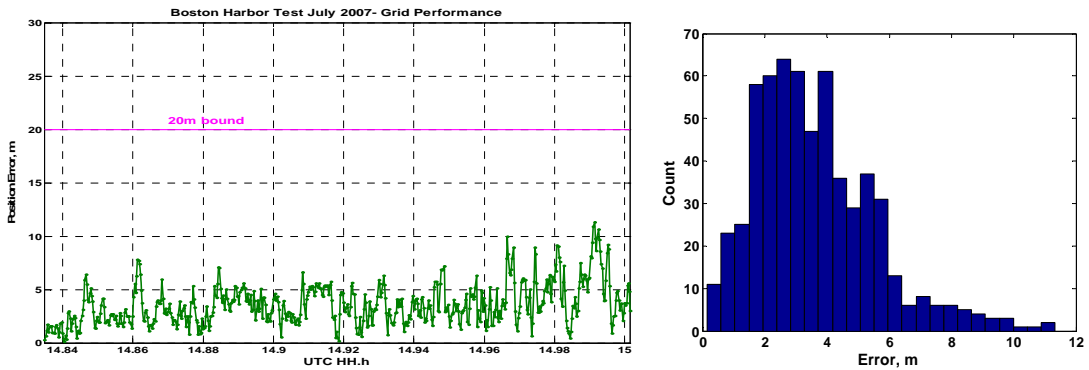


Figure 33: Accuracy results for the Boston harbor segment: left, error versus time; right, histogram of errors.

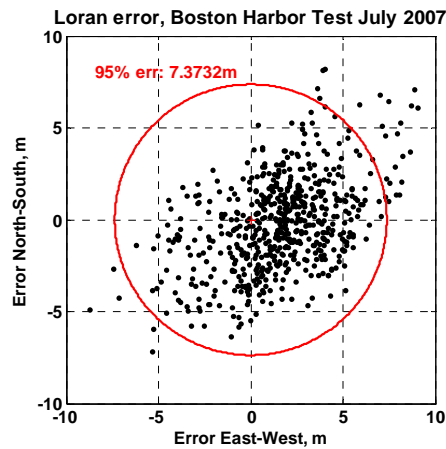


Figure 34: Error scatter for Boston harbor test showing sub 18m error 95% of the time.

TEMPORAL CORRECTIONS

The second important component of the harbor *e*Loran strategy is the broadcasting of the temporal component. The system architecture currently implemented is shown in Figure 35¹. Seasonal Monitor sites located near various harbors make local ASF measurements and transmit the Loran data back to a server located at CGA at one minute intervals. This server archives the data for long-term analysis and also provides a way to monitor the status of the monitors. A second process on the server takes the monitor site ASF, subtracts the reference value for the site (differences from a reference value are transmitted in order to reduce the number of bits needed since LDC is low data rate system), formats the data for transmission on the LDC, and then uploads the data as a file to an FTP server located at the Loran Support Unit in Wildwood, NJ (LSU). Each Loran station retrieves the data for the Monitor Sites to be transmitted from the server and then broadcasts the temporal ASF corrections over the LDC.

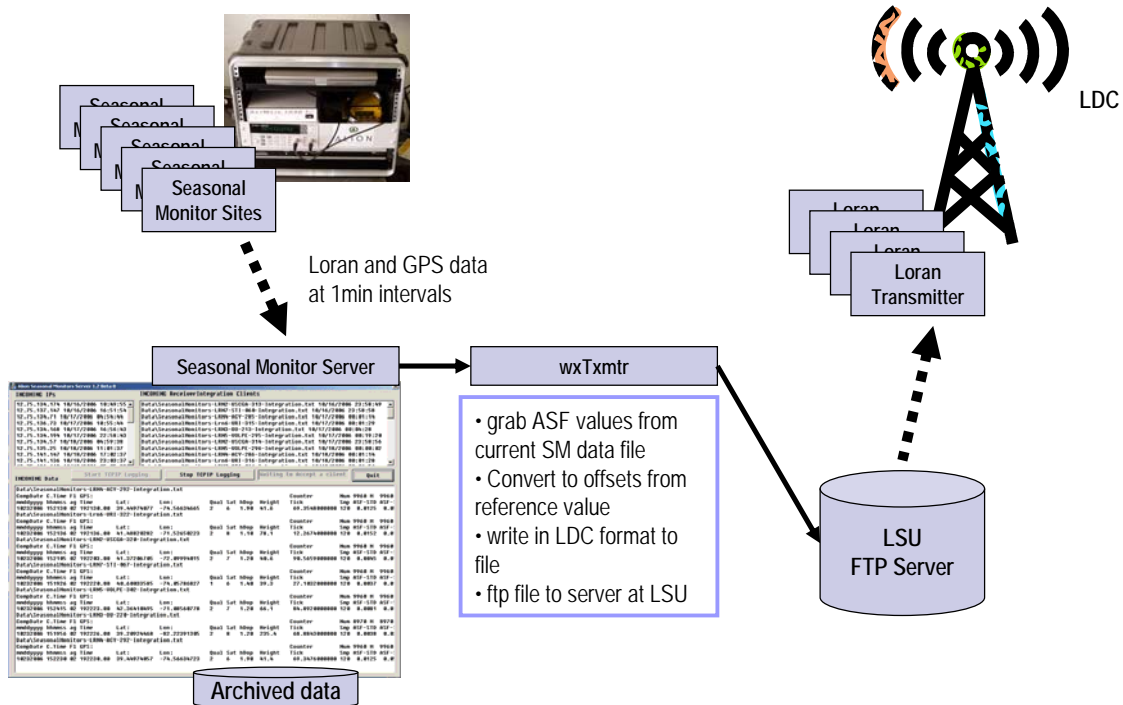


Figure 35: LDC architecture.

The messages are queued up and transmitted from each tower in a repeating sequence. A typical message sequence is shown in Figure 36. The sequence is a Time message followed by an Almanac message followed by ASF messages from two monitor sites (6 messages per site), then Time, Almanac, two monitor sites, etc. In this case, since there are an odd number of sites being broadcast, the last grouping only has one set of monitor site messages. Each message is 45 bits long and takes 24 symbols to transmit with the current LDC coding scheme. More detailed information about the LDC message format can be found in [9]. Since 1 symbol is transmitted for each group of Loran pulses, at the GRI of 8970 for Seneca (the station used for the *e*Loran demonstration) it takes about 2.15 seconds per message and about 2.3 minutes to transmit the entire cycle of 64 messages. Since there are five Time messages sent in the cycle of 64 messages, a time update is provided every 27.5 seconds. This latency in the ASF messages could be a problem in the future and is under investigation.

¹ Work is in progress on defining the architecture for the long-term (implemented system).



Figure 36: Typical LDC message sequence.

CONCLUSIONS / FUTURE WORK

In conclusion, we have described our current methodology for *eLoran* HEA positioning. Our approach to computing the spatial ASF grids from survey data yields workable grids; the noise in the ASF measurements gets averaged out in the grid creation process so that measurement noise is not an issue. Also, our work indicates that a 500m grid spacing is typically sufficient; smaller spacing is only necessary if dictated by the physical size of the HEA area. In addition the harbor survey methodology has been established and proven.

For the temporal ASF component we have shown that having the correct temporal value is critical to meeting HEA accuracy. The current approach for real-time broadcast works; however, we need to resolve time latency and transmission issues. Currently under investigation is the required frequency and filtering of the differential corrections and the required monitor site spacing (see [10] for additional insight on this issue). In areas where geometry and/or signal strength are poor, the receiver performance becomes critical. Also, the H-field antenna characterization and calibration are also very important for an *eLoran* receiver.

ACKNOWLEDGMENTS

The authors would like to recognize the support of the rest of the Alion New London team (M. Wiggins and K. Dykstra), the captains and crews of the Coast Guard Auxiliary vessels (*Launch #5* in New York, *Myst* in New London, *Halcyon Lace* in Norfolk and *Three J's* in Boston) and the C. G. Loran Support Unit (CDR Chris Nichols and LT Chris Dufresne) who is the sponsor of this work.

DISCLAIMER AND NOTE

The views expressed herein are those of the authors and are not to be construed as official or reflecting the views of the U.S. Coast Guard, Federal Aviation Administration, or any agency of the U.S. Government.

BIOGRAPHIES

Gregory Johnson is a Senior Program Manager at Alion Science & Technology. He heads up the New London, CT office which provides research and engineering support to the Coast Guard Academy and the USCG R&D Center. He has a BSEE from the USCG Academy (1987), a MSEE from Northeastern University (1993), and a PhD in Electrical Engineering from the University of Rhode Island (2005). Dr. Johnson is a member of the Institute of Navigation, the International Loran Association, the Institute of Electrical and Electronics Engineers, and the Armed Forces Communications Electronics Association. He is also a Commander in the Coast Guard Reserves.

Richard Hartnett holds the grade of Captain in the U. S. Coast Guard, and has served on the faculty of the Engineering Department at the U.S. Coast Guard Academy (USCGA) since 1985. He graduated from the USCGA with his BSEE in 1977, and earned his MSEE from Purdue in 1980 and his PhD in Electrical Engineering from the University of Rhode Island in 1992. He is the 2004 winner of the International Loran Association Medal of Merit.

Peter Swaszek is a Professor in the Department of Electrical, Computer, and Biomedical Engineering at the University of Rhode Island. He received his Ph.D. in Electrical Engineering from Princeton University. His research interests are in signal processing with a focus on digital communications and navigation systems. Prof. Swaszek is a member of the Institute of Electrical and Electronics Engineers, the Institute of Navigation, the International Loran Association, and the American Society of Engineering Education. He is spending the 2007-08 academic year on sabbatical at the USCGA.

REFERENCES

- [1] "Enhanced Loran (eLoran) Definition Document," International Loran Association Version 0.1, 12 January 2007.
- [2] "Loran's Capability to Mitigate the Impact of a GPS Outage on GPS Position, Navigation, and Time Applications," Prepared for the Federal Aviation Administration, Vice President for Technical Operations, Navigation Services Directorate 31 March 2004.
- [3] R. Hartnett, G. Johnson, and P. Swaszek, "Navigating Using an ASF Grid for Harbor Entrance and Approach," presented at the Institute of Navigation, Annual Meeting, Dayton, OH, 6 - 9 June 2004.
- [4] M. Kuhn, G. Johnson, P. Swaszek, *et al.*, "Warping Time and Space: Spatial Correlation of Temporal Variations," presented at the 35th Annual Technical Symposium, International Loran Association, Groton, CT, 24-25 October 2006.
- [5] P. Swaszek, G. Johnson, R. Hartnett, *et al.*, "Methods for Developing ASF Grids for Harbor Entrance and Approach," presented at the 35th Annual Technical Symposium, International Loran Association, Groton, CT, 24-25 October 2006.
- [6] G. W. Johnson, P. F. Swaszek, R. Hartnett, *et al.*, "A Procedure for Creating Optimal ASF Grids for Harbor Entrance & Approach," presented at the ION GNSS 2006, Fort Worth, TX, 26 - 29 September 2006.
- [7] G. W. Johnson, P. F. Swaszek, R. Hartnett, *et al.*, "Navigating Harbors at High Accuracy Without GPS: eLoran Proof-of-Concept on the Thames River," presented at the Institute of Navigation, National Technical Meeting, San Diego, CA, 22 - 24 January 2007.
- [8] G. W. Johnson, P. F. Swaszek, R. Hartnett, and C. Nichols, "Navigating Harbors at High Accuracy without GPS: eLoran in the United States," presented at the European Navigation Conference GNSS 2007, Geneva, Switzerland, 31 May 2007.
- [9] K. Dykstra and B. B. Peterson, "The Loran Data Channel: Progress to Date and Future Plans," presented at the 35th Annual Technical Symposium, International Loran Association, Groton, CT, 24-25 October 2006.
- [10] P. F. Swaszek, G. W. Johnson, S. C. Lo, *et al.*, "An Investigation into the Temporal Correlation at the ASF Monitor Sites," presented at the Annual Symposium, International Loran Association (ILA-36), Orlando, FL, 16-17 October 2007.